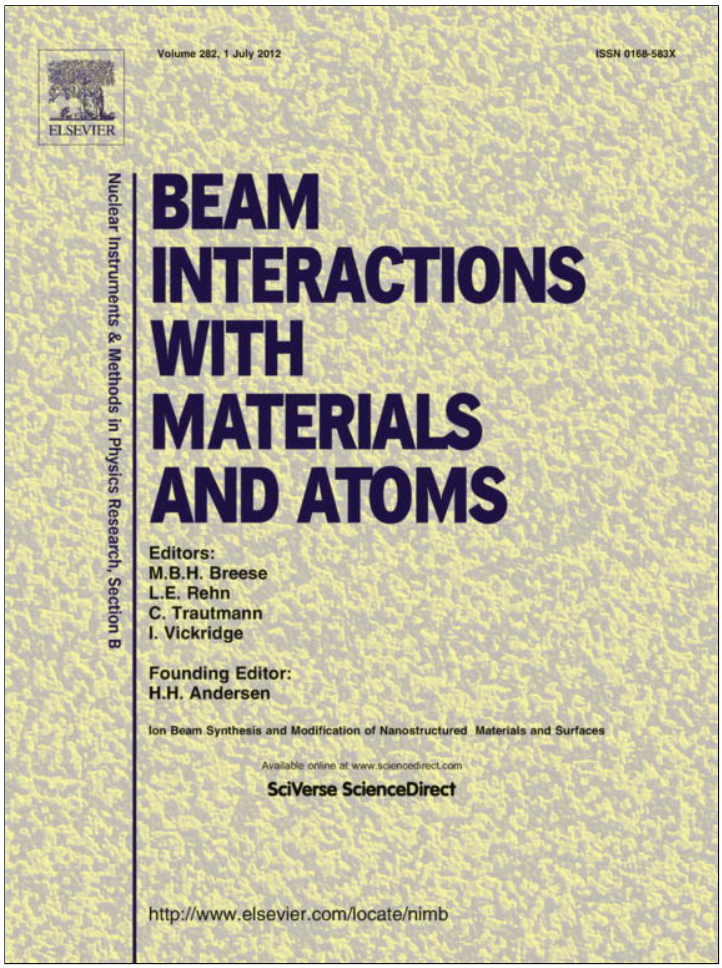

Nuclear Instruments and Methods in Physics Research B 282 (2012) 112–115

Contents lists available at SciVerse ScienceDirect

Nuclear Instruments and Methods in Physics Research B

journal homepage: www.elsevier.com/locate/nimb

Impact of keV-energy argon clusters on diamond and graphite

V.N. Popok [a,b,*], J. Samela [c], K. Nordlund [c], V.P. Popov [d]

[a] Institute of Physics, University of Rostock, Universitätplatz 3, 18051 Rostock, Germany
[b] Department of Physics and Nanotechnology, Aalborg University, Skjernvej 4A, 9220 Aalborg Ø, Denmark
[c] Department of Physics and Helsinki Institute of Physics, University of Helsinki, P.O. Box 43, 00014 Helsinki, Finland
[d] Institute of Semiconductor Physics, Lavrentieva Av. 13, 630090 Novosibirsk, Russia

ARTICLE INFO

Article history:
Available online 16 September 2011

Keywords:
Cluster ion implantation
Craters
Hillocks
Scanning probe microscopy
Molecular dynamics simulations

ABSTRACT

Impact of keV-energy size-selected Ar_n (n = 16, 27, 41) cluster ions on diamond and graphite is studied both experimentally and by molecular dynamics simulations. For the case of diamond, relatively high cluster kinetic energies (above certain threshold) are required to produce severe radiation damage and originate crater formation on the surface. This is related to very strong chemical bonds and both the melting (or sublimation) point and thermal conductivity of diamond being the highest among the solids. For the case of graphite, which is layered material with weak van der Waals bonds between the graphene planes, significant radiation damage is already introduced by impact of clusters with low kinetic energies (a few tens of eV/atom). However, collisions of the argon clusters cause very elastic response of the graphene planes that leads to efficient closure of the craters which could be formed at the initial stage of impact.

1. Introduction

Nowadays, there are a lot of activities worldwide focused on controlling and modifying the physical and chemical properties of materials on the nanoscale. One of the possible approaches is the use of cluster ion beams. This method gives advantages in control of cluster size and cluster-surface impact energy which are of significant importance for a number of practical applications [1,2]. From this point of view, it is essential to clearly understand all the phenomena occurring during the cluster interaction with matter. However, for the case of energetic clusters there is no commonly accepted theory of stopping, i.e. simulations and experiments demonstrate different dependences of the depth of cluster penetration and radiation damage on the implantation conditions. In particular, the cluster-impact-induced damage and related phenomena like crater and hillock formation [3–5] are of interest because the mechanisms of these effects are key points for understanding of fundamental physical aspects of the energetic cluster–matter interaction.

In this paper, we present results of keV-energy argon cluster impact on graphite and diamond, two different allotropes of carbon. Graphite is of interest as a model material with atomically smooth surface, on which even tiny defects can be resolved. Moreover, it is a layered material with rather strong covalent bonds in the graphene planes but very weak bonding between them. This type of structure brings some specificity into the cluster stopping [6]. Although diamond is also an allotropic form of carbon, it has rather different crystalline structure and is known as a material with the strongest chemical bonds and unique mechanical properties. Some of its electronic characteristics, for instance, the high mobility of electrons and holes, low noise and leakage current and extremely high thermal conductivity make this material attractive for high-power and high-frequency electronics [7]. Diamond also is a potential platform of solid-state quantum devices [8].

2. Experimental

Small plates (with area from a few up to 100 mm^2 and thickness of ca. 1 mm) of (1 1 1) synthetic diamond and highly ordered pyrolytic graphite (HOPG) were used for the experiments. The samples were implanted by Ar_n^+ cluster ions using the facilities PUCLUS and CIDA [9,10]. A typical mass-spectrum of the clusters is presented in Fig. 1. One of the diamond samples was bombarded by an entire spectrum of cluster sizes (n is from 1 up to ca. 80 atoms) accelerated up to 4 keV/cluster. Other diamond plates were implanted by size-selected $Ar_{27\pm2}^+$ cluster ions with energies of 9, 12 and 15 keV/cluster ($E_{at} \approx 333$, 444, 555 eV/atom, respectively). HOPG samples were bombarded by Ar_n^+ with $n = 16 \pm 1$ and 41 ± 2. The mean kinetic energies varied from 1.6 up to 16.0 keV/cluster. The implantation fluencies were kept at ca. 10^{10} cm^{-2} for all cases.

The samples were studied *ex situ* by scanning tunnelling microscopy (STM) and atomic force microscopy (AFM) using a NanoLaboratory Ntegra-Aura (from NT-MDT). The STM studies

* Corresponding author at: Institute of Physics, University of Rostock, Universitätplatz 3, 18051 Rostock, Germany.
E-mail address: vp@nano.aau.dk (V.N. Popok).

0168-583X/$ - see front matter © 2011 Elsevier B.V. All rights reserved.
doi:10.1016/j.nimb.2011.08.055

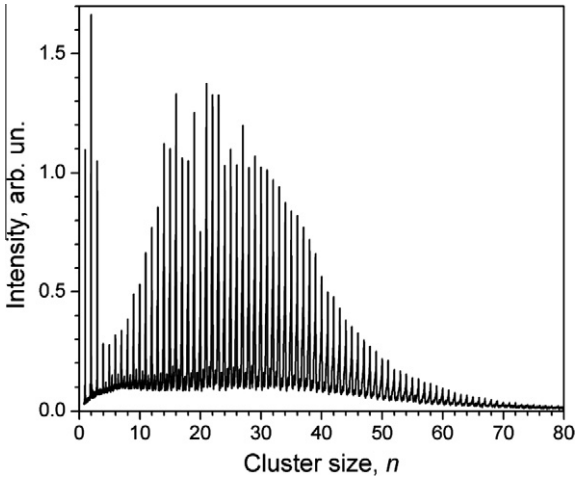

Fig. 1. Typical mass-spectrum of Ar_n^+ cluster ions.

were carried out in constant current mode with a bias of 70–80 mV using PtIr tips. AFM measurements were done in tapping mode using commercial ultrasharp Si and DLC cantilevers with curvature radius of the tip ca. 2–3 nm.

Classical molecular dynamics (MD) simulations were performed using Parcas simulation software [11] and the Tersoff interatomic potential [12,13]. A Lennard–Jones type pair potential was used between the Ar atoms. A short-range repulsive force [14] was also present between all pairs of atoms to better describe collisions between them. The Ar–C interaction was purely repulsive [15,16]. The size of the (1 1 1) diamond target in the simulations was 20 × 20 × 10 nm. The borders of the target were cooled and the simulations were run until the impact area was cooled to the ambient temperature of 300 K (15–25 ps depending on the cluster energy). Five simulations were performed at each of the energies in the interval between 3 and 21 keV/cluster varying the initial orientation and position of the impacting Ar_{27} cluster. Details on MD simulations of argon cluster implantation in graphite can be found elsewhere [17].

3. Results and discussion

It has been shown both experimentally and by simulations that impact of energetic clusters on various materials can cause formation of craters or hillocks [1–6,18]. In our case, bombardment of diamond by the 4 keV clusters did not lead to any observable changes of the surface topography in AFM images. As one can see in Fig. 1, the maximum of intensity of the cluster beam corresponds to sizes around 20–30 atoms that gives mean kinetic energies of about 130–200 eV/atom. These values are above the threshold energy (between 35 and 80 eV) needed to displace a carbon atom in diamond [19]. However, the density of the energy deposited at the impact spot is too low to cause significant local excavation of material, i.e. crater formation, or melting followed by the liquid flow and hillock formation especially taking into account extremely high melting point of diamond (ca. 3820 K). Another important point to consider is that diamond melts only at high pressures otherwise it sublimes at about 3900 K. Simulations have shown that cluster-surface collision leads to the compression of material at initial stage of impact and the pressure can locally rise up to a GPa level [3,18]. Thus, a formation of diamond liquid phase on impact of small argon clusters is possible but only on a short time scale. Our MD simulations show that impacts of the clusters with the above-mentioned low energies do not induce a considerable liquid zone. Radiation damaged areas are very small and there are no craters formed (Fig. 2(a)). Since typical root mean square value of roughness of pristine diamond surfaces used in our experiments was about 0.15–0.25 nm (500 × 500 nm areas), these small damaged spots can hardly be registered by AFM.

Similar results (small damage formation) were obtained elsewhere for Ar_{60} colliding on a diamond surface with an energy of 200 eV/atom [20]. For the case of 100 keV Ar_{961} clusters ($E_{at} \approx 104$ eV/atom), the impact areas were larger in diameter due to the bigger clusters but the damaged surface looked quite smooth [21]. It was calculated that the temperature can exceed the melting (or sublimation) point of diamond only in the very core of the impact area and the heat rapidly dissipates towards bulk due to high thermal conductivity. Thus, there was not liquid flow

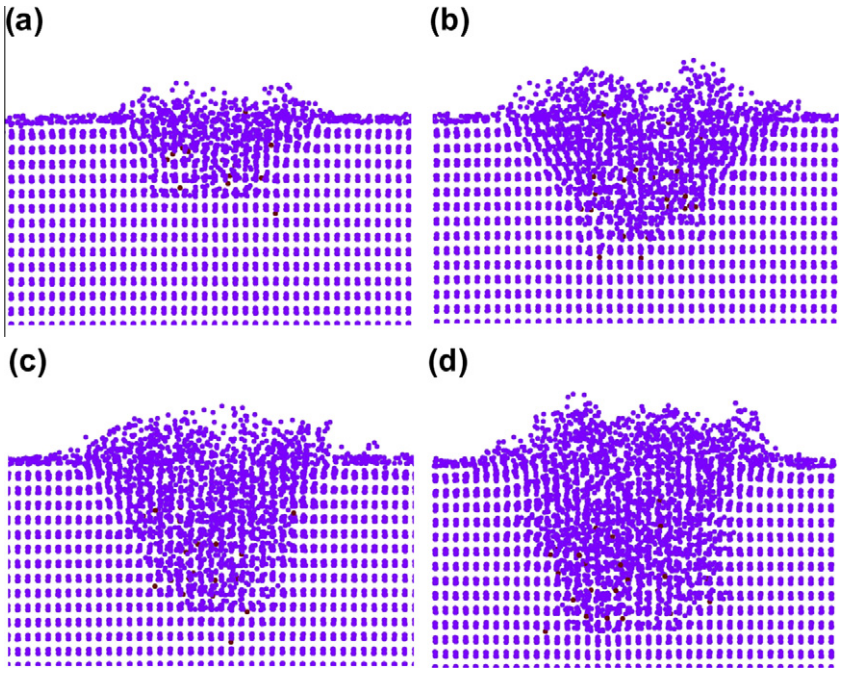

Fig. 2. Snapshots of MD simulations (after 15 ps). Impact of Ar_{27} clusters on diamond with energies of (a) 111 eV/atom, (b) 333 eV/atom, (c) 444 eV/atom and (d) 666 eV/atom. Width of the frames is 5 nm, thickness of the cross-section is 2 nm.

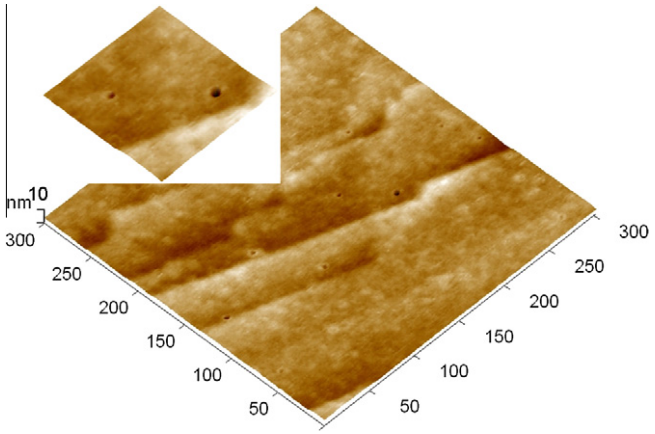

Fig. 3. AFM image of diamond surface implanted by Ar_{27}^{+} cluster ions with energy of 12 keV (ca. 444 eV/atom). Insert shows enlarged central part of the image with craters.

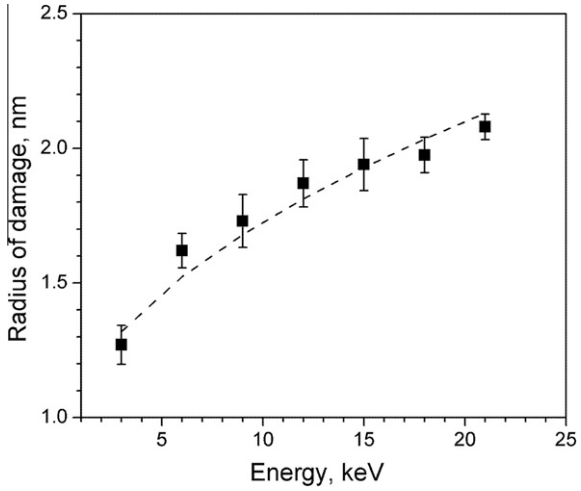

Fig. 4. Dependence of radius of damaged diamond area on cluster kinetic energy. Dashed line is the best fit, $0.83 + 0.28E^{1/2}$.

phenomenon which could lead to pronounced craters with rims. For the formation of significant damage in the form of craters or hillocks higher kinetic energies above a certain threshold value are required as, for instance, was shown for the case of sapphire bombarded by Ar_n and Xe_n clusters [5].

Increase of the cluster kinetic energy leads to severe damage of diamond as one can see in Fig. 2(b–d) presenting snapshots of MD simulations. The damaged regions do not contain cavities which are typical to crater formation in many other materials. This is an indication that no liquid flow occurs in this case after the impact even at energies up to 21 keV/cluster (ca. 777 eV/atom). The cluster bombardment of diamond causes craters only through direct sputtering of the surface atoms. Experimentally, it is found that the bombardment of 9 and 12 keV Ar_{27}^{+} cluster ions leads to the formation of small hillocks with height of 0.5–2.0 nm and basal diameter of 10–15 nm. In a few cases the craters of 5–7 nm in diameter are observed (Fig. 3). The surface density of the bumps and craters correlates well with the fluence. It is worth noting that the pits with diameters of ca. 5 nm are the smallest ones which can be resolved by the used cantilevers. Craters with smaller rim-to-rim diameters will be imaged as bumps due to the tip convolution effect [22]. Thus, the measured hillocks most probably represent either unresolved very small craters or tiny bumps of the damages areas. This suggestion is supported by modelling which does not predict liquid flow phenomena. Hence, there is a very low probability for the formation of hillocks caused by local melting of the materials and subsequent expansion as, for example, for silicon [22]. MD simulations also show that mean diameters of the craters (or damaged areas) are about 3–4 nm for the energies of 9–15 keV/cluster (Fig. 4), thus, below the lateral resolution of AFM for craters. In the simulations, crater radii scale as $E^{1/2}$ (Fig. 4). For not very high cluster energies used in our case, shape of the damaged areas is close to hemispherical (Fig. 2), i.e. radius of the damaged area is approximately equal to its depth. Hence, we can assume that the depth of radiation damage also scales as $E^{1/2}$. This is an important finding because the square root of energy is proportional to the cluster momentum and, as suggested earlier for implantation of graphite, the stopping power is a linear function of momentum [17,23]. Thus, despite the significant difference in the structure and properties of diamond and graphite, there seems to be a general correlation between the mechanisms of cluster stopping in these two materials. However, this question requires further investigation.

Contrary to diamond, the damaged areas can be imaged on HOPG using STM even for very low cluster kinetic energies. This is caused by much lower displacement energies in graphite (ca. 12–20 eV along *c*-axis) [24]. One of the typical images showing nanoscale bumps on the surface is presented in Fig. 5(a). The cluster impact introduces significant damage to the depth of a few graphene layers (Fig. 5(b)) that locally changes the structure and electronic properties and as a result the tunnelling current during the STM measurements. Lateral dimensions of the bumps measured by STM correlate well with those of the simulated damaged areas.

Compared to diamond, clear craters are never observed in HOPG on the impact of Ar_{16} and Ar_{41} clusters within the studied keV -energy interval. The experimental results found their explanation through MD simulations. Graphite has a layered structure with

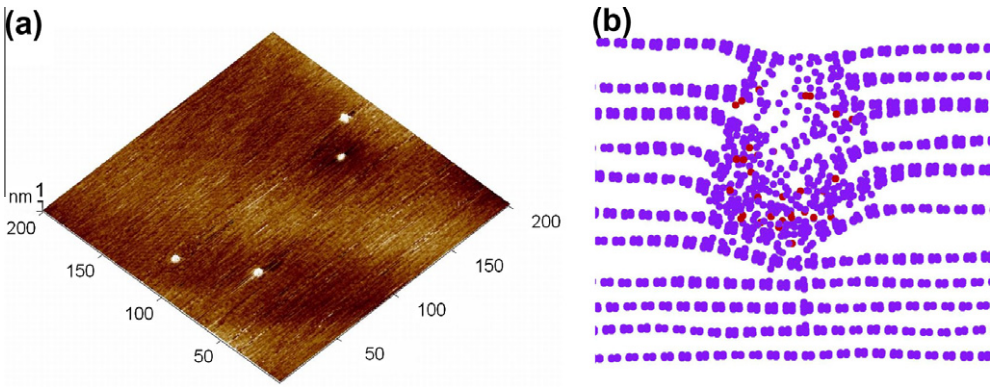

Fig. 5. (a) STM image of HOPG surface implanted by Ar_{41}^{+} cluster ions with energy of 4.1 keV (100 eV/atom) and (b) snapshot of MD simulation (after 20 ps) for the same impact conditions. Width of the frame is 5 nm and it shows 1 nm thick slice.

strong covalent bonds in the plane and very weak (van der Waals) ones between the planes. Therefore, the graphite structure responds very elastically to cluster impact: the collision induces oscillations of the graphene planes [6]. The oscillations have very little influence on the structure outside the immediate impact region with primary displacement cascades, although their amplitude could be as large as the distance between two neighbouring planes. Thus, a crater can be formed only at the initial stage of impact. The elastic behaviour of graphene sheets at a later stage causes efficient closure of the craters and only disordered areas are finally formed as shown in Fig. 5. It is worth noting that Ar_n cluster impact on HOPG can lead to the formation of well-pronounced craters [25]. However, the cluster should be larger and they should have high kinetic energies in order to be able to provide high energy density transfer to the graphite target.

4. Conclusions

Radiation damage in diamond and graphite on impact of keV-energy argon clusters is studied both experimentally and by MD simulations. For the case of diamond, it is shown that crater formation on the cluster impact requires relatively high kinetic energies (above certain threshold) that is related to very strong chemical bonds, the greatest melting and sublimation points as well as the highest thermal conductivity. The craters are formed by direct sputtering. There is no liquid flow phenomenon detected which could lead to pronounced crater rim formation or appearance of hillocks. Contrarily, for the case of graphite, significant radiation damage can be introduced on impact of clusters with low kinetic energies (a few tens of eV/atom). However, there is no crater formation found on impact of relatively small clusters used in the current experiments. MD simulations demonstrate very elastic response of the graphene planes to cluster impact: the collision induces oscillations which have very little influence on the structure outside the immediate impact region with primary displacement cascades. Such behaviour leads to efficient closure of the craters which could be formed at the initial stage of impact.

References

[1] N. Toyoda, I. Yamada, IEEE Trans. Plasma Sci. 36 (2008) 1471.
[2] V.N. Popok, Mater. Sci. Eng. R 72 (2011) 137.
[3] L.P. Allen, Z. Insepov, D.B. Fenner, C. Santeufemio, W. Brooks, K.S. Jones, I. Yamada, J. Appl. Phys. 92 (2002) 3671.
[4] K. Nordlund, T.T. Järvi, K. Meinander, J. Samela, Appl. Phys. A 91 (2008) 561.
[5] S.V. Prasalovich, V.N. Popok, P. Person, E.E.B. Campbell, Eur. Phys. J. D 36 (2005) 79.
[6] J. Samela, K. Nordlund, J. Keinonen, V.N. Popok, E.E.B. Campbell, Eur. Phys. J. D 43 (2007) 181.
[7] C. Raynaud, D. Tournier, H. Morel, D. Planson, Diamond Relat. Mater. 19 (2010) 1.
[8] A.D. Greentree, B.A. Fairchild, F.M. Hossain, S. Prawer, Mater. Today 11 (9) (2008) 22.
[9] V.N. Popok, V.S. Prasalovich, M. Samuelsson, E.E.B. Campbell, Rev. Sci. Instrum. 73 (2002) 4283.
[10] S. Vučković, M. Svanqvist, V.N. Popok, Rev. Sci. Instrum. 79 (2008) 073303.
[11] K. Nordlund, M. Ghaly, R.S. Averback, M. Caturla, T.D. De la Rubia, J. Tarus, Phys. Rev. B 57 (1998) 7556.
[12] J. Tersoff, Phys. Rev. Lett. 61 (1988) 2879.
[13] J. Tersoff, Phys. Rev. B 37 (1988) 6991.
[14] J.F. Ziegler, J.P. Biersack, M.D. Littmark, The Stopping and Ranges of Ions in Matter, Lulu Press, Morrisville, 2008.
[15] K. Nordlund, J. Keinonen, T. Mattila, Phys. Rev. Lett. 77 (1996) 699.
[16] K. Nordlund, N. Runeberg, D. Sundholm, Nucl. Instrum. Meth. Phys. Res. B 132 (1997) 45.
[17] V.N. Popok, J. Samela, K. Nordlund, E.E.B. Campbell, Phys. Rev. B 82 (2010) 201403(R).
[18] T.J. Colla, R. Aderjan, R. Kissel, H.M. Urbassek, Phys. Rev. B 62 (2000) 8487.
[19] J.F. Prins, T.E. Derry, J.P.F. Sellschop, Phys. Rev. B 34 (1986) 8870.
[20] T. Aoki, J. Matsuo, G. Takaoka, I. Yamada, Mater. Res. Soc. Symp. Proc. 650 (2001) R3.40.1.
[21] Y. Yamaguchi, J. Gspann, Phys. Rev. B 66 (2002) 155408.
[22] J. Samela, K. Nordlund, V.N. Popok, E.E.B. Campbell, Phys. Rev. B 77 (2008) 075309.
[23] S. Pratontep, P. Preece, C. Xirouchaki, R.E. Palmer, C.F. Sanz-Navarro, S.D. Kenny, R. Smith, Phys. Rev. Lett. 90 (2003) 055503.
[24] F. Banhart, Rep. Prog. Phys. 62 (1999) 1181.
[25] S. Houzumi, K. Mochiji, N. Toyoda, I. Yamada, Jpn. J. Appl. Phys. 44 (2005) 6252.